

Effect of Pulse Reverse electrodeposition Parameters on the Microstructure of the Ni/NiO Composite Coating

Ping Wang¹, Changxuan Wang¹, Yanli Wang^{1,*}, Shenghua Zhang^{2,3}, Weihua Li^{4,*}

¹ School of Chemistry and Chemical Engineering, Guangxi University, Nanning, 530004, P R China.

² Guangxi Key Laboratory of Processing for Nonferrous Metallic and Featured Materials, Nanning, 530004, Guangxi, P R China.

³ School of Resources, Environment and Materials, Guangxi University, Nanning, 530004, P R China.

⁴ College of Chemical Engineering and Technology, Sun Yat-sen University, Zhuhai, 519082, P R China.

*E-mail: wyl15104008565@126.com, liweihua@qdio.ac.cn

Received: 7 September 2019 / Accepted: 18 October 2019 / Published: 30 November 2019

In this paper, a Ni/NiO composite coating has been prepared by the pulse reverse current (PRC) plating technique and the effects of parameters including average current density, pulse frequency, total duty cycle, forward duty cycle, plating temperatures and NiO content on the micro-morphology of the composite coating has been investigated. The results reveal that the composite coating prepared at an average current density of $10 \text{ A}\cdot\text{dm}^{-2}$, a pulse frequency of 100 Hz, total duty cycle of 80%, forward duty cycle of 60%, plating temperature of 50 °C and $50 \text{ g}\cdot\text{L}^{-1}$ of NiO addition exhibit a smooth and dense structure, with uniformly distributed NiO particles.

Keywords: Pulse reverse plating, electrodeposition parameter, Ni/NiO composite coating, molten fluorides.

1. INTRODUCTION

The molten fluoride salt is a new kind of desirable medium for heat transfer and storage ediums in the field of high-temperature industrial applications, such as molten salt reactor (MSR), spent fuel reprocessing and aluminium electrolysis. Molten fluorides have unique thermal chemical properties and thermal physical properties such as high heat capacity and heat conductivity, excellent radiation stability, low neutron capture cross section and low viscosity [1]. However, the molten fluorides at high operating temperatures between 500 and 900 °C show strong corrosiveness. Structural materials are prone to be corroded through the active dissolution of alloy elements into the melt [2]. To improve the corrosion resistance of materials in molten fluorides, one of the most effective methods is to

prepare coatings on the surface of matrix. Ni is a metal with excellent chemical stability in molten fluoride. Olson et. al.^[3] reported that Ni coating can significantly improve the corrosion resistance of Cr-containing alloys in molten fluorides. However, the single Ni coating cannot inhibit the external diffusion of Cr and other elements in alloys and the formation of voids during long-term immersion in molten fluorides. Therefore, adding a diffusion barrier between Ni coating and matrix alloy to inhibit the external diffusion of Cr from the matrix alloy can significantly improve the corrosion resistance of Ni coating in molten fluoride. Metallic oxides, such as Cr₂O₃ [1] and Al₂O₃ [4], have shown great potential for inhibiting the mutual diffusion of elements between the substrate and the Ni coating due to the fact that the diffusion coefficient of Cr and Fe in the oxide ceramics is smaller than that in the Ni [1,5,6].

At present, physical vapor deposition (PVD) [7, 8], thermal pre-oxidation growth^[9] and in-situ growth [1,4] are commonly used to prepare oxide diffusion barriers. However, the micro-defects of the coatings prepared by PVD are unavoidable. And the obtained coating is in physical bonding with the substrate, which is detrimental during the long-term service of the coating [10]. Compared with PVD, the pre-oxidation thermal growth and in-situ growth methods can form a chemical bonding between oxide coating and substrate, which can significantly improve the adhesion of the coating. Xu et al. prepared Al₂O₃ [4] diffusion barrier in cold-sprayed NiCrAlY/Ni multilayered coatings on 304SS substrate by in-situ thermal growth method. Cold-sprayed Ni(O) composite coating between the substrate and the upper NiCrAlY/Ni coating is made to supply the active O during the formation of Al₂O₃ diffusion barrier. Xu et al. also reported an in-situ grown Cr₂O₃ [1] diffusion barrier between cold-sprayed Ni coating and the 310SS substrate. The oxygen source for the growth of Cr₂O₃ diffusion barrier is still from the cold-sprayed Ni(O) composite coating. They found that both the Al₂O₃ and Cr₂O₃ diffusion barriers could effectively prevent the diffusion of Fe and Cr from the substrate to the Ni layer. However, unconnected interfaces or micro-structures are inevitably existed in the Ni(O) composite coating prepared by cold spray technology, which can be easily transmitted to the subsequent formed diffusion barrier, resulting in the decreasing of the diffusion resistance property for the diffusion barrier in the long-term service. Therefore, how to obtain continuous, dense diffusion barriers with good chemical bonding between matrix and outer Ni layer is the key question to prepare coatings in molten fluorides.

In our paper, the composite layer is prepared by pulse electroplating technology, which can uniformly incorporated the metal oxide particles NiO into the Ni coating to supply the oxygen needed during the in-situ formation of Cr₂O₃ diffusion barrier with some advantages over the cold spray such as establishing a coat with the decreased internal stress, controlled composition, decreased porosity[11]. In the pulse electroplating process, different parameters can affect the microstructure [12], alloy compositions [13] and crystalline morphologies [14] of the composite layer, which in turn affect the microstructure and property of the Cr₂O₃ diffusion barrier. Therefore, the main aim of the present study is to employ pulse reverse electroplating to produce a Ni/NiO composite layer on a 316L substrate. The effects of duty cycle, forward duty cycle, frequency and deposition temperature on the composition distribution, structure and morphology of Ni/NiO composite layer will be explored. Other investigations such as the diffusion barrier effect and corrosion resistance property of the coatings will be further reported in the new future.

2. EXPERIMENTAL PROCEDURES

A type 316L stainless steel was used as the substrate, whose composition is shown in Table 1. The bulk metals were cut into samples with a size of 10 mm × 15 mm × 2 mm by an electric spark cutter, followed by grinding down to 600 grit SiC paper and ultrasonic cleaning in acetone for 5 minutes, rinsing with distilled water.

The electrolyte for the electrodeposition of the outer Ni layer was composed of 250 g·L⁻¹ NiSO₄·6H₂O, 40 g·L⁻¹ NiCl₂·6H₂O, 40 g·L⁻¹ H₃BO₃, 0.3 g·L⁻¹ C₁₂H₂₅SO₄Na, 2 g·L⁻¹ C₇H₅O₃NS. The pH of the electrolyte was about 4. The acidic plating solution can prevent the agglomeration of metallic ions, which is beneficial to reduce the grain size [15]. For the electrodeposition of the inner Ni/NiO composite layer and specific contents of particles of pure NiO (99.9%) with the values of 10, 20, 50 and 100 g·L⁻¹ were added to the above electrolyte using ultrasonic dispersion for 1 h to ensure a good dispersion of NiO particles. The particle size of the NiO powders used in this experiment is not uniform, with a range of about 50-100 nm, as shown in Fig. 1. All solutions were prepared by analytical reagents and deionized water. The deposition electrolyte was stirred during the electrodeposition of Ni/NiO composite layer using a magnetic stirrer to maintain the suspension of the nanoparticles added in the bath [16].

In this paper, the pulse reverse current (PRC) electrodeposition was performed to obtain the Ni/NiO composite coating in a two-electrode system using a Pt electrode as the counter electrode and the prepared 316L stainless steel as the working electrode. The waveform of the PRC electrodeposition in the experiment is shown in Fig. 2, in which the J_{av} represents the average current density, J_+ positive peak current density, J_- reverse peak current density, t cycle time, t_{on} positive pulse time, t'_{on} reverse pulse time, t_{off} stop time, and t'_{off} reverse stop time, respectively. The total cycle time was 200 s in all cases during pulse plating. The parameters for the PRC electrodeposition are shown in Table 2. For the electrodeposition of outer Ni layer, the average current density J_{av} was set to 3.5 A·dm⁻², the bath temperature was kept at 45 °C, the frequency f was fixed at 100 Hz, the duty cycle was set to 40 %, and the positive duty cycle was kept at 36%.

Table 1. Nominal chemical composition of the substrate (in wt.%).

element	C	Si	Mn	P	S	Ni	Cr	Mo
content	≤0.03	≤1.00	≤2.00	≤0.035	≤0.03	12.0-15.0	16.0-18.0	2.0-3.0

In order to explore the effects of average current density, duty cycle, forward duty cycle, frequency and electroplating temperature on the microstructure of Ni/NiO composite layer, the electrodeposition of the inner Ni/NiO composite layer was designed with the following parameters: (1) Frequency of 50, 100, 500, 2000 Hz at fixed average current density (10 A·dm⁻²), electroplating bath temperature (50 °C), duty cycle (80 %) and forward duty cycle (60 %). (2) Electroplating bath

temperature of 45, 50, 55, 60 °C at fixed average current density (10 A·dm⁻²), frequency (100 Hz), duty cycle (80 %) and forward duty cycle (60 %). (3) Duty cycle of 50, 70, 80, 90 % and forward duty cycle of 40, 60, 80, 90 % at fixed average current density (10 A·dm⁻²), frequency (100 Hz), electroplating bath temperature (50 °C).

Scanning electron microscope (SEM) was used to characteristic the composite coatings.

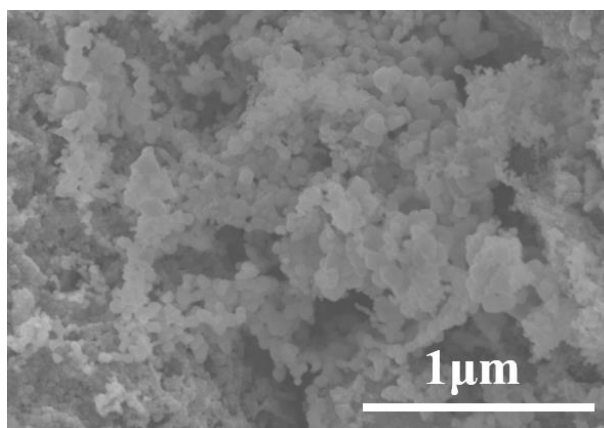


Figure 1. The surface morphology of the NiO particles used in this experiment.

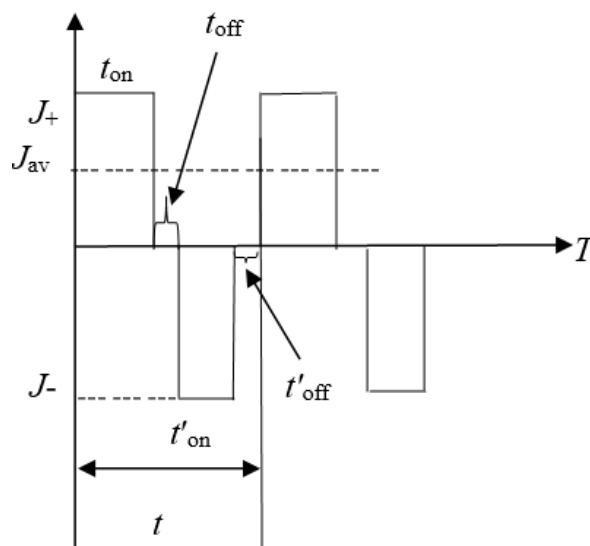


Figure 2. Wave profile of the pulse reverse current (PRC) electrodeposition.

Table 2. Operating parameters of pulse reverse current (PRC) electrodeposition.

	t_{on} (ms)	t_{off} (ms)	t'_{on} (ms)	t'_{off} (ms)
PRC plating	4.8	3.2	0.8	1.2

3. RESULTS AND DISCUSSION

3.1 Effects of pulse frequencies

Fig. 3 indicates the effect of pulse frequency on the morphology of the Ni/NiO composite layer. As the figures show the Ni/NiO) composite coating prepared under the 100 Hz has compact, flat surface and uniform microstructure (Fig. 3b). The surface of the coating becomes denser and, and the dispersion of the NiO particles tends to more even when the c pulse frequency increases from 50 Hz up to 100 Hz. As the NiO grains become more spherical and more dispersed due to an increase in the pulse frequency [17-19]. While the pulse frequency increases from 100 Hz up to 2000 Hz, the agglomeration of the NiO particles become more obvious and the surface of the coating becomes rougher. Form Fig. 3d, it can be seen that when the frequency is extremely high, the surface is very rough with large nodular and cauliflower shaped morphology and large areas of NiO particle agglomeration, which can be related to the high deposition rate of NiO particles.

The higher the pulse frequency is, the more the numbers of periodic positive and negative discharges per unit time and instantaneous peak current density are. As a result, loosely adsorbed particles are easily removed by hydrodynamic forces before they are embedded in the coating. In this way, the application of reverse pulse technique cannot achieve the expected promotion effect in terms of changes in the electrodeposited morphology, and hindering the particles embedded in the coating and making the coating rougher. On the other hand, if the number of periodic discharges is too few, the chances of particles entering the coating will be very small, thus the content of incorporated particles will be also reduced. In the process of pulse electroplating, the frequency reduction is closer to DC polarization, which is not conducive to the compactness and smoothness of the coating [17]. It can result in a tapered morphology on the surface of the coating, as shown in Fig. 3a.

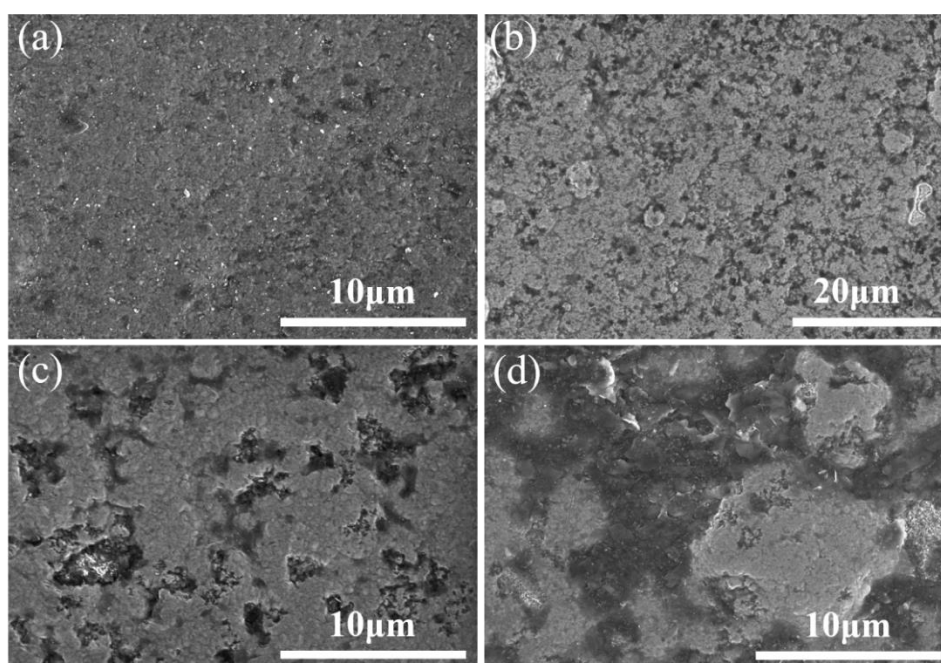


Figure 3. Surface morphologies of the as-deposited Ni/NiO composite layer at different pulse frequencies: (a) 50 Hz, (b) 100 Hz, (c) 500 Hz, (d) 2000 Hz.

3.2 Effects of total and forward duty cycles

Fig. 4 shows the Ni/NiO morphologies at different total pulse duty cycles of 50, 70, 80, and 90%, while maintaining other conditions are the same. As shown in Fig. 4, when the total duty cycle is 80%, the surface of the obtained coating is flat and compact with no obvious holes (Fig. 4c). Furthermore, the particles are evenly distributed. However, when the duty ratio is too large or too small, the surface morphology of the obtained coating is not ideal, with increased roughness (Fig. 4a and b) and formed micro-holes (Fig. 4d). This can be attributed to the fact that the parameter t_{on} of the current density increases with the increased duty cycle [20]. And the corresponding electrodeposition is increased and the incorporated NiO particles is also increased, the deposited coatings gradually become flat and dense. However, if the duty cycle is too high, the metal ions precipitated in the cathode cannot be timely supplemented within a relatively short time, resulting in a reduction in the density of the obtained coating and the existence of holes. Similarly, if the duty ratio is too small and the t_{off} time is too long, the metal ions consumed on the cathode surface have been replenished and the system has returned to a stable state [21]. At that point, the extension of time is meaningless.

Furthermore, we also investigated the effect of the forward duty cycle on the microstructures of deposited Ni/NiO composite coating. Fig. 5 illustrates the surface morphologies of the obtained coatings deposited by continuous variations of forward duty cycle (from 40 % to 90 %) at the fixed total duty cycle of 80%. The white particles on the surface indicate the presence of non-conductive NiO particles in the coating [22]. It presents that when the forward duty cycle is kept at 40%, the SEM micrograph exhibits a nodular structure with some micro-poles. When the forward duty cycle is further increased to 60 %, the surface smoothness is increased, the nodular structure and the uniformity of the distribution of NiO particles is refined. However, when the forward duty cycle increases to 80 %, the SEM micrograph transfers from nodular structure to needle-like morphology [17,23]. Furthermore, the aggregation of the incorporated NiO particles is evident. Some pin-holes and unevenly distributed NiO particles are also found at forward duty cycle of 90 %. Therefore, the optimum value of forward duty cycle is 60 %.

The changes of surface morphology can be ascribed that, with the increasing of forward duty cycle, the peak current density increases, the electrodeposition processes of Ni^{2+} and NiO particles are enhanced [24]. At the same time, the dissolution rate of the coating is accelerated by the reverse pulse current, and some particles with large particle size will be desorption from the surface of the electrode, making the surface smooth and fine. However, excessive extension of duty cycle makes the power supply mode of pulse power supply similar to that of DC power supply. The obtained coating will show rough surface, the particle distribution is extremely uneven, and even a small number of holes exist, as shown in Fig 5c and d, which may be due to that Ni^{2+} and NiO particles consumed at cathode cannot replenished at some extent during the short anodic pulse working time.

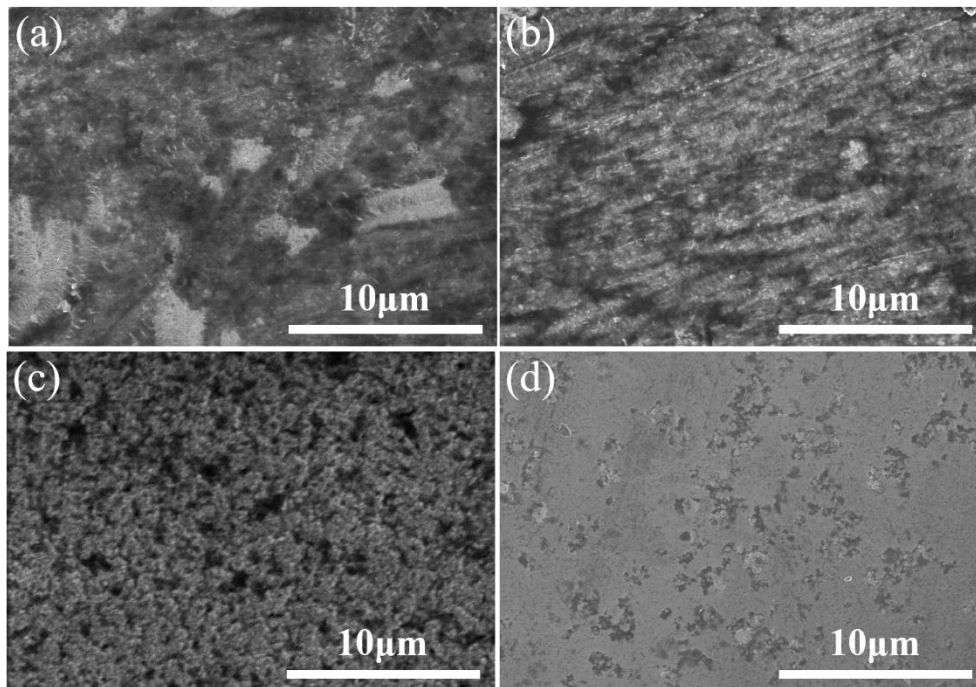


Figure 4. Surface morphologies of the as-deposited Ni (NiO) composite coatings at different duty cycles: (a) 50 %, (b) 70 %, (c) 80 %, (d) 90 %.

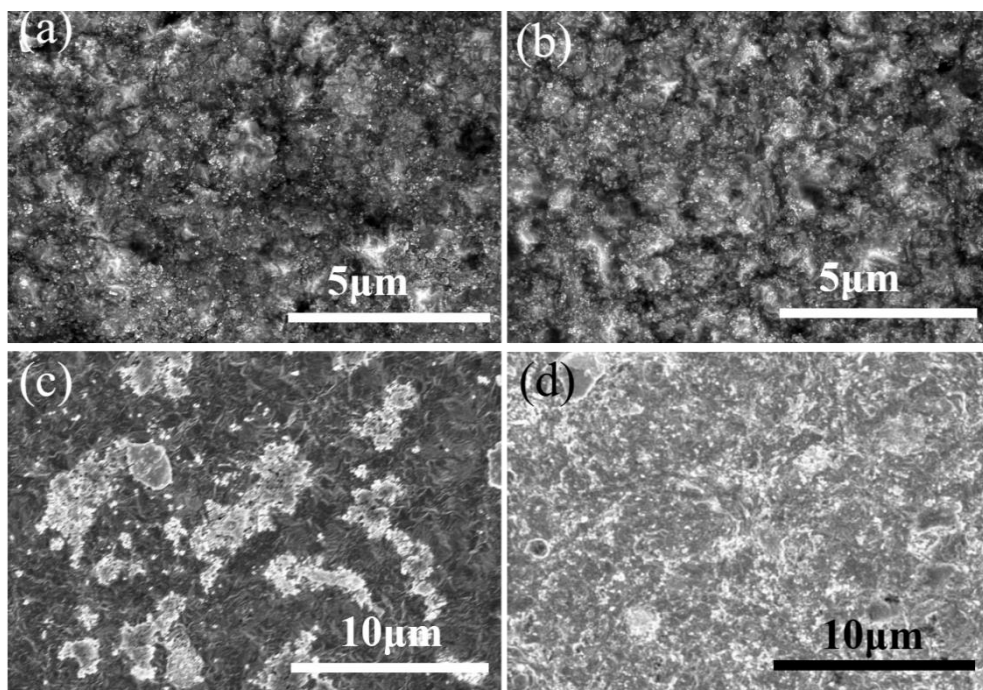


Figure 5. Surface morphologies of the as-deposited Ni (NiO) composite coatings under different forward duty cycles: (a) 40 %, (b) 60 %, (c) 80 %, (d) 90%.

3.3 Effects of the plating temperature

The surface morphologies of the specimen prepared at different plating temperatures of Ni/NiO composite coatings are shown in Fig. 6. As can be seen from the figure, temperature is another key

factor affecting the quality of the coating. With the increase of temperature, the concentration of particles involved in the reaction increases, the diffusion rate increases, and the content of particles entering the coating increases, which leads to the compactness of the coating [25-27]. When the temperature is set at 50 °C, the obtained composite coating is smooth and dense, with uniformly distribution of NiO particles. While the temperature is increased gradually to 60 °C, the surface of the coating gradually becomes loose and even crack appears, as shown in Fig. 6c and d, which may be due to the intensification of hydrogen evolution reaction and polarization of electrodes.

Guglielmi [28] proposed the famous two-step adsorption model: weak adsorption and strong adsorption are two stages in the composite electroplating process. The diffusion dynamics and adsorption model can be used to explain the nanocomposite electroplating process in our experimental process with temperature as the main influencing factor. By increasing the bath temperature, the movement of particles in the solution increases and the probability of collision among particles will also be increased. Thus, the adsorption of particles on the cathode can be improved and the nucleation rate is increased. However, the phenomenon of hydrogen evolution will also become more and more serious with the increasing temperature, resulting in that the surface of the plating layer is rougher, even with cracks.

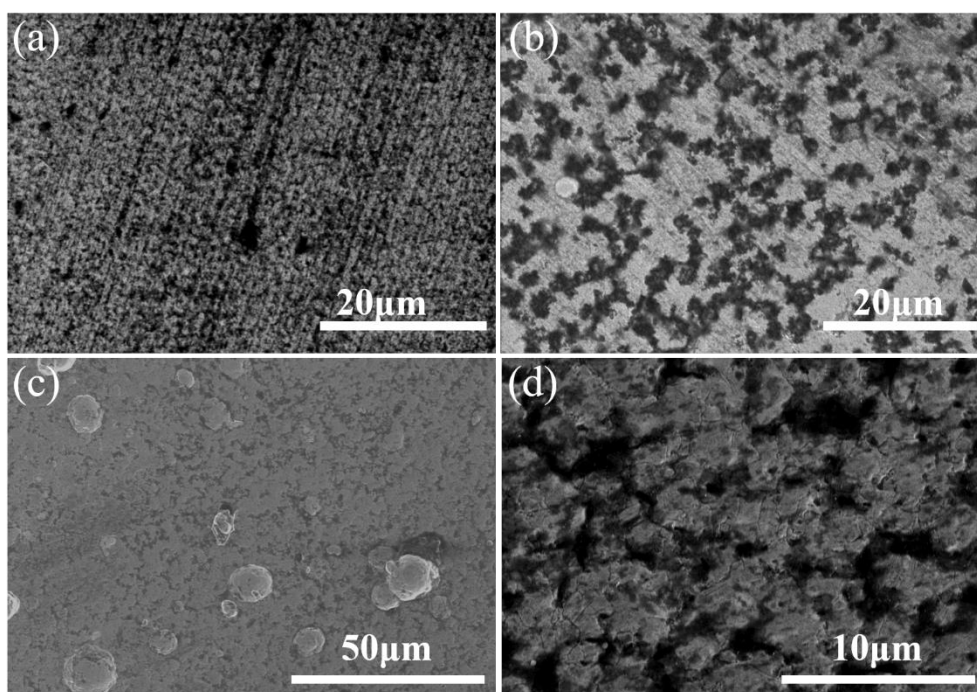


Figure 6. Surface morphologies of the as-deposited Ni (NiO) composite coatings at different plating temperatures: (a) 45 °C, (b) 50 °C, (c) 55 °C, (d) 60 °C.

3.4 Effects of NiO addition

As the final purpose of the preparation of Ni/NiO) composite coating is to supply sufficient oxygen resources for the subsequent in-situ grown of Cr₂O₃ diffusion barrier. Therefore, the effect of

the NiO particles content in electroplating solution on the preparation of Ni/NiO composite coating is studied. In Fig. 7, the morphologies of Ni/NiO composite coatings are presented under different NiO powder additions. It can be observed that by gradually increasing powder additions from 10 to 100 $\text{g}\cdot\text{L}^{-1}$, the flatness of Ni/NiO composite coating increases firstly and then decreases. Increasing the concentration of particles in the plating bath is beneficial to the formation of dense and uniform thick coatings.^[27] Particularly, the surface shows a large number of cellular structures in Fig. 7d at 100 $\text{g}\cdot\text{L}^{-1}$ of NiO in the bath solution, which seriously affect the uniformity and compactness of the coating.

According to MTM [29] theory, during particles deposition process under pulse-reverse electroplating technique, NiO nanoparticles are absorbed to suitable sites by interfacial electric field force and hydrodynamic. If there are too many particles in the solution, the ion reduction rate adsorbed on the surface of the particles cannot keep up with the embedding speed of the particles in the coating, which will lead to the particles cannot co-deposit with nickel ions. Furthermore, the adsorption capacity of the cathode surface is limited. With the further increase of particle concentration, the adsorption capacity of the particles on the cathode surface will be weakened, and the particles can be taken away easily by the flowing electroplating solution, leading to the reduction of particle content in the coating and the surface of the coating becomes rough [30]. By comparing the morphology of Ni/NiO composite coatings with the same magnification, it can be concluded that 50 $\text{g}\cdot\text{L}^{-1}$ of NiO in the plating solution results in a spherical and denser morphology, which can be ascribed to the proper number of nucleation sites.

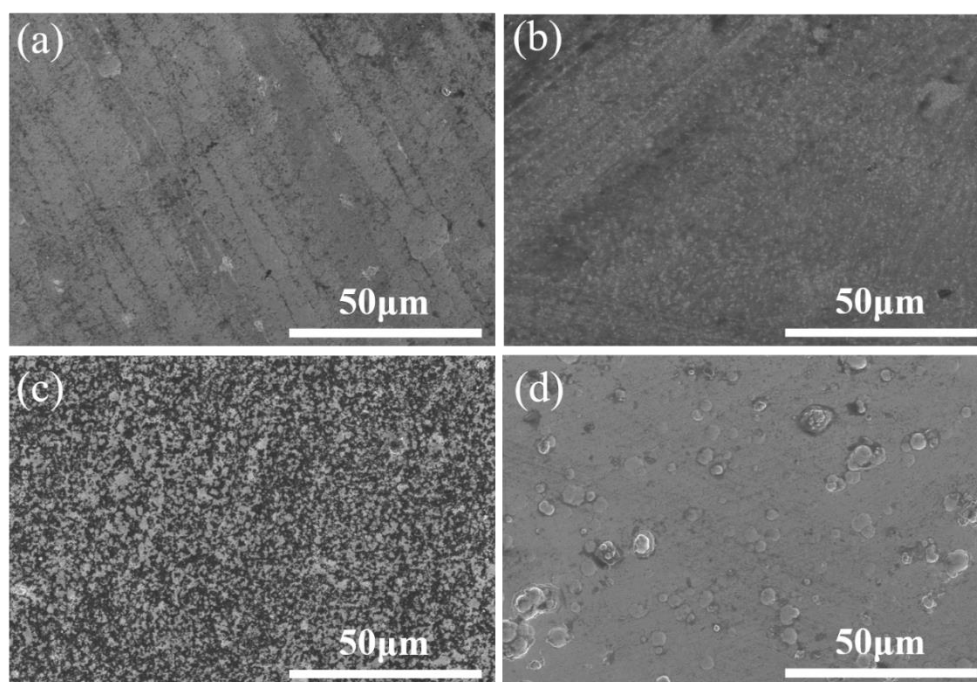


Figure 7. Surface morphologies of the as-deposited Ni/NiO composite coatings under different NiO particles addition: (a) 10 $\text{g}\cdot\text{L}^{-1}$, (b) 20 $\text{g}\cdot\text{L}^{-1}$, (c) 50 $\text{g}\cdot\text{L}^{-1}$, (d) 100 $\text{g}\cdot\text{L}^{-1}$.

4. CONCLUSIONS

A Ni/NiO composite coating has been electrodeposited by pulse electrodeposition. The following conclusions can be drawn from this study: the pulse frequency, duty cycle, temperature and particle content have dual effect on the smoothness of the surface and the uniformity of particle distribution. As these parameters increase in a range, there is an optimal value. The optimized PRC electrodeposition parameters of Ni/NiO composite coating at the constant current density of $10 \text{ A}\cdot\text{dm}^{-2}$ are obtained: the total duty cycle is 80%, the positive duty cycle is 60%, the pulse frequency is 100 Hz, and the bath temperature is $50 \text{ }^\circ\text{C}$.

ACKNOWLEDGEMENTS

This project is supported by National Natural Science Foundation of China [Grant No. 51801035], Natural Science Foundation of Guangxi Province [Grant No. 2018GXNSFBFA138059], the open foundation of Guangxi Key Laboratory of Processing for Non-ferrous Metals and Featured Materials, Guangxi University [Grant No. GXYSOF1812] and the Basic Competence Improvement Project for Middle and Young Teachers in the Guangxi Zhuang Autonomous Region [Grant No. 2018KY0031].

References

1. Y.X. Xu, X.T. Luo, C.X. Li, G.J. Yang and C.J. Li, *J. Therm. Spray. Technol.*, 25 (2016) 526.
2. B.J. You, *Ph.D. Thesis, Hsinchu: National TsingHua Univiversity*, (2010)1.
3. L. Olson, K. Sridharan, M. Anderson and T. Allen, *J. Nucl. Mater.*, 411 (2011) 51.
4. Y.X. Xu, M. Chirol, C.J. Li and A. Vardelle, *Surf. Coat. Technol.*, 307 (2016) 603.
5. R.K. Wild, *Corros. Sci.*, 17(1977)87.
6. I. Sato, M. Takaki, T. Arima, H. Furuya, K. Idemitsu, Y. Inagaki, M. Momoda and T. Namekawa, *J. Nucl. Mater.*, 304 (2002) 21.
7. Y. X. Cheng, W. Wang, S. L. Zhu, L. Xin and F. H. Wang, *Intermetallics*, 18 (2010) 736.
8. H. Peng, H. Guo, R. Yao, J. He and S. Gong, *Vacuum*, 85 (2010) 627.
9. Z. Xu, L. He, R. Mu, R. Mu, X. Zhong and X. Cao, *Vacuum*, 82 (2011) 1251.
10. Q.M. Wang, Y.N. Wu, M.H. Guo, P.L. Ke, J. Gong, C. Sun and L. S. Wen, *Sur. Coat. Technol.*, 197 (2005) 68.
11. F. Khorashadizade, H. Saghafian and S. Rastegari, *J. Alloy. Compd.*, 770 (2019) 98.
12. P. Gyftou, E.A. Pavlatou and N. Spyrellis, *Appl. Surf. Sci.*, 254 (2008) 5910.
13. S.K. Ghosh, *Surf. Coat. Technol.*, 126 (2000) 48.
14. S. Ruan and C.A. Schuh, *Acta. Mater.*, 59 (2009) 3810.
15. J. Man, S. Zhang, J.F. Li, B. Zhao and Y. Chen, *Surf. Coat. Technol.*, 249 (2014) 118.
16. S.R. Allahkaram, M.H. Nazari, S. Mamaghani and A. Zarebidaki, *Mater. Design.*, 32 (2011) 750.
17. Y.Y. Yang, Y.N. Li and M. Pritzker, *Electrochim. Acta.*, 213 (2016) 225.
18. A.M. El-Sherik, U. Erb and J. Page, *Surf. Coat. Technol.*, 88 (1997) 70.
19. D. Zhu, W.N. Lei, N.S. Qu and H.Y. Xu, *CIRP Ann. Manuf. Technol.*, 51 (2002) 173.
20. Z.M. Ding, Q. Y. Feng and J.M. Song, *T. Mater. Heat. Treat.*, 33 (2012) 129.
21. K.H. Hou and I.B. Huang, *Mater. Chem. Phys.*, 80 (2003) 662.
22. Y. Len, *John. Wiley. & Sons.*, (2009)1.
23. A.T. Miller, B.L. Hassler and G.G. Botte, *J. Appl. Electrochem.*, 42 (2012) 925.
24. G. Roventi, R. Fratesi and R.A. Della, *J. Appl. Electrochem.*, 30 (2000) 173.
25. W.P. Wu, J.W. Liu, Y. Zhang, X. wang and Y. Zhang, *J. Appl. Electrochem.*, 49 (2019) 1043.
26. H. Natter and R. Hempelmann, *J. Phys. Chem.*, 100 (1996) 19525.

27. R.Hessam and P.Najafisayar, *Int. J. Hydrogen. Energ.*, 44 (2019) 2851.
28. N. Guglielmi, *J. Electrochem. Soc.*, 119 (1972) 1009.
29. W.Y. Tu, B.S. Xu and S.Y. Dong, *China Surf. Eng.*, 4(2003)1.
30. H.Matsubaba, Y.Abe and Y.Chiba, *Electrochim. Acta.*, 52 (2007) 3047.

© 2020 The Authors. Published by ESG (www.electrochemsci.org). This article is an open access article distributed under the terms and conditions of the Creative Commons Attribution license (<http://creativecommons.org/licenses/by/4.0/>).